UC Berkeley
UC Berkeley Previously Published Works

Authors
Orlandi, Manuel
Coelho, Jaime AS
Hilton, Margaret J
et al.

Peer reviewed

Parametrization of Non-covalent Interactions for Transition State Interrogation Applied to Asymmetric Catalysis

Manuel Orlandi,[†] Jaime A. S. Coelho,[‡] Margaret J. Hilton,[†] F. Dean Toste,*,[‡] and Matthew S. Sigman*,[†]

[†]Department of Chemistry, University of Utah, 315 South 1400 East, Salt Lake City, Utah 84112, United States
[‡]Department of Chemistry, University of California, Berkeley, California 94720, United States

S Supporting Information

ABSTRACT: The use of computed interaction energies and distances as parameters in multivariate correlations is introduced for postulating non-covalent interactions. This new class of descriptors affords multivariate correlations for two diverse catalytic systems with unique non-covalent interactions at the heart of each process. The presented methodology is validated by directly connecting the non-covalent interactions defined through empirical data set analyses to the computationally derived transition states.

Figure 1. Computed energies $E\pi$ and distances $D\pi$ as parameters. (A) General idea and $\pi-\pi$ sandwich complex. (B) T-shaped complex. (C) Determination of weighted parameters.

Selectivity in chemical reactions and specifically in catalytic processes is commonly a complex function of various non-covalent interactions (NCIs) occurring prior to or at the transition state (TS). Although the determination and quantification of such interactions is highly desirable in order to predict and understand reaction performance, this is a difficult goal using purely empirical observations, as NCIs are often low-energy (0−2 kcal/mol) and dynamic.[1] In this vein, computational analysis of TSs can provide insight into significant influences in the selectivity-determining step(s).[2] However, as is always a consequence of TS interrogation, a detailed understanding of the roles of all reaction components is obligatory.

Considering this, we have reported a complementary physical organic strategy that uses multidimensional linear regression (MLR) to compare specific structural descriptors to the observed output for reactions with ambiguous mechanistic possibilities.[3] This methodology provides prediction for reaction optimization and mechanistic insights on the basis of the parameters used.[3a,4−8] However, a key limitation to date has been the limited number of suitable parameters to describe attractive NCIs.[2b,9,10] Therefore, a more precise parameter set is required to define these essential underlying phenomena, which occur in a wide swath of processes. Herein we introduce computed π-stacking/CH−π interaction energies and distances as parameters in multivariate correlation analysis (Figure 1). As described below, this strategy can also link the statistical models to computationally derived TS analysis to reveal the ensemble of NCIs responsible for effective catalysis.

The interactions of π systems, which constitute a core set of NCIs invoked in catalytic processes, have been the subject of extensive experimental and computational studies.[2b,9,11,12] In particular, Houk and Wheeler have reported comp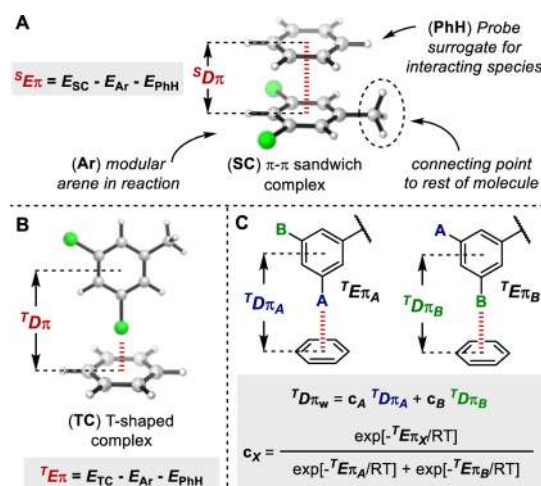uted interaction energies of numerous sandwich and parallel-displaced arene dimers (Figure 1A), which linearly correlate with the Hammett σ_m parameter.[13] These reports inspired us to compute representative interaction energies ($E\pi$) and distances ($D\pi$, defined as the distance between the centers of the two interacting moieties) to be used as descriptors for putative π interactions (Figure 1A,B). In particular, $D\pi$ is dependent on both distinct geometric and electronic features, since it is influenced by the attractive energy as well as the substituent size. Moreover, when an NCI can occur in more than one conformer, the associated properties can be weighted according to their energies, as depicted in Figure 1C; the obtained parameters are represented as $E\pi_w$ and $D\pi_w$. For the two case studies presented below, the relevant complexes were calculated at the B97-D/def2TZVP level of theory, since this functional paired with a triple-ζ basis set has been reported to be a practical, economical compromise for computing NCIs.[14]

In order to test our hypothesis, we examined the kinetic resolution of chiral benzylic alcohols reported by Birman and co-workers[15] (Figure 2A), in which π stacking was demonstrated to be a controlling element in the computed TSs (Figure 2B).[16] In addition, sufficient data spanning a significant range of measured
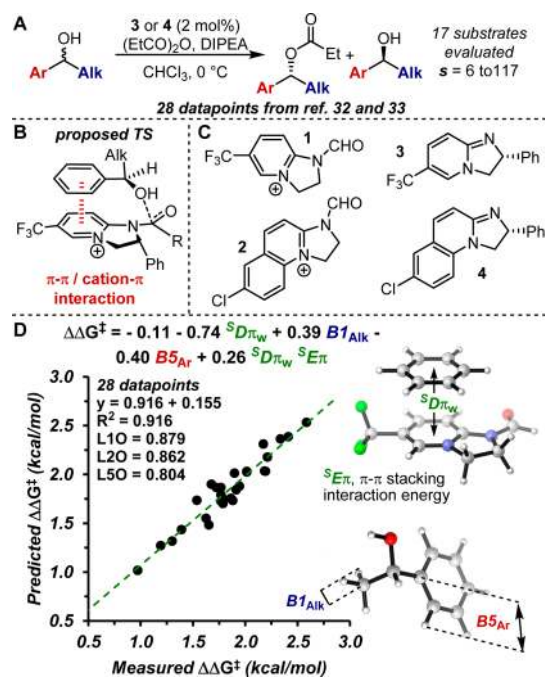
Figure 2. Proof-of-concept reaction system. (A) Birman's kinetic resolution of benzyl alcohols. (B) Proposed/computed transition state. (C) Simplified structures (**1** and **2**) used as mimics for acylated catalysts **3** and **4**, respectively. (D) Mathematical model.

selectivity factors (*s* from 6 to 117, $\Delta\Delta G^{\ddagger}$ from 0.97 to 2.58 kcal/mol) were reported, which is required for developing statistically sound models (see the Supporting Information (SI) for details).[15,16] Parameter collection was initiated by computing 28 unique $\pi-\pi$ sandwich complexes between the aryl/alkenyl groups and model systems **1** and **2**, which represent the cationic acylated catalysts **3** and **4** used in the reaction (Figure 2C). To simulate a π-stacking interaction, the two arenes were aligned in a parallel orientation at a defined distance, centering the interacting arene with the pyridinium ring in **1** or **2**. Subsequently, the distance between the rings was optimized, resulting in the minimum energy for the stacked conformation, $^{S}E\pi$, at distance $^{S}D\pi$ (Figures 2D and S1A). When additional conformers were possible, the formula in Figure 1C was applied, affording $^{S}E\pi_{w}$ and $^{S}D\pi_{w}$ as weighted parameters to account for the possibility of dynamic interactions (see the SI).

Initial evaluation of these parameters revealed a single-parameter correlation between $^{S}D\pi_{w}$ and the selectivity factor *s*, represented as the $\Delta\Delta G^{\ddagger}$ value ($R^2 = 0.70$; Figure S4), which supports the presence of a stacked $\pi-\pi$ interaction in the TS. After application of MLR to interrogate additional effects on the reaction's selectivity, the model reported in Figure 2D was identified ($R^2 = 0.92$), effectively describing 28 data points with three additional terms: the Sterimol parameters[8] $B1_{Alk}$ (alkyl substituent's minimum width) and $B5_{Ar}$ (aryl substituent maximum width) and the cross term $^{S}D\pi_{w}{}^{S}E\pi_{w}$. Cross-validation methods are consistent with a statistically sound model (see the leave-*K*-out (LKO) values). Examination of each term's coefficient in the model suggests that the reaction's enantio-selectivity is most influenced by the π-stacking interaction (represented by the terms $^{S}D\pi_{w}$ and $^{S}D\pi_{w}{}^{S}E\pi_{w}$) followed by steric effects, consistent with previous studies.[16]

After evaluating our new π parameters for mechanistic rationalization of a well-studied reaction, we sought to test whether they can also be applied to a system for which the

specific interactions occurring in the TS have not yet been determined. Hence, the second case study for the application of these π parameters was the enantiodivergent fluorination of allylic alcohols previously reported by our teams (Figure 3A).[17]
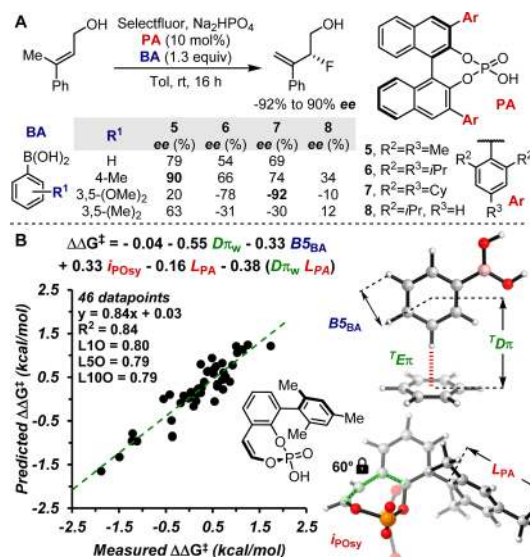

Figure 3. Enantiodivergent fluorination of allylic alcohols. (A) Reaction scheme and substituent effects of BAs and PAs on the enantioselectivity. (B) Multivariate model correlating the stereoselectivities from catalysts **5–8** and 18 different BAs.

In this process, the allylic alcohol and the boronic acid (BA) condense to form a mixed boronic ester, which is proposed to coordinate via H-bonding with the chiral phosphate anion (PA).[17b] From this complex, the enantioselective electrophilic fluorination occurs. Notably, the enantioselectivity ranges from -92 to $+90\%$ ee when various combinations of PAs and BAs are applied, reflecting a $\Delta\Delta G^{\ddagger}$ range of 3.5 kcal/mol. Thus, this reaction is highly sensitive to NCIs involved in enantioselectivity-controlling events. Despite extensive mechanistic studies that provide support for the general reaction mechanism,[17b] a clear representation of the likely NCIs responsible for the enantioselectivity has not been elucidated. In this context, previous attempts to correlate all of the measured enantiose-lectivities through MLR were unsuccessful.

Two key observations provided a framework to initiate interrogation of this system: (1) meta-substituted BAs lead to inverted enantioselectivity compared with other substitution patterns on the BA, and (2) the sensitivity toward the BA substitutions is amplified when PAs **5–7** containing substituents at the 2- and 6-positions are employed (Figure 3A). On this basis, it was hypothesized that a T-shaped π interaction between the BA and the PA may occur in the TS.[17b] Therefore, T-shaped complexes were calculated in a similar manner as described previously, using a perpendicular orientation of the probe, benzene, and the BA's meta positions (Figure 1B). $^{T}E\pi_{w}$ and $^{T}D\pi_{w}$ for the T-shaped dimers were calculated for a set of 18 BAs. Preliminary analysis of the enantioselectivity data resulting from each BA with PA **6** revealed a good correlation with a single parameter, $^{T}D\pi_{w}$ ($R^2 = 0.77$; Figure S5A), which supports that T-shaped interactions are relevant in the TS.

As a next step, we sought to develop a comprehensive model by integrating different combinations of BAs and PAs (46 data points; see the SI). Additional parameters to describe the PA
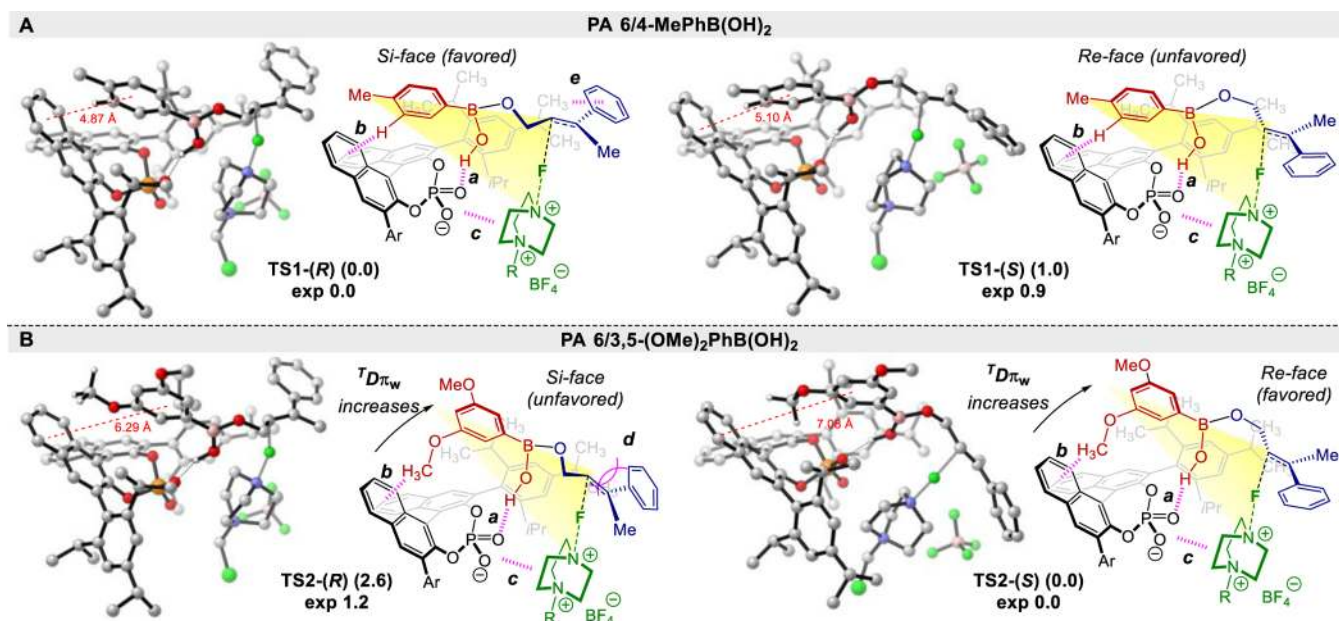
Figure 4. Structures and relative free energies (in kcal/mol) of the low-lying TSs for (A) PA **6**/4-MePhB(OH)$_2$ and (B) PA **6**/3,5-(MeO)$_2$PhB(OH)$_2$. Energies were computed at the ωB97X-D/def2-TZVPP/SMD(toluene) level of theory on the ωB97X-D/6-31G(d) geometries. Nonrelevant hydrogen atoms have been omitted for clarity.

catalysts, such as IR stretching frequencies and Sterimol values, were acquired using a simple model system (Figure 3B; see the SI). The parameters include $^TD\pi_w$, accounting for geometric requirements derived from the apparent presence of a π interaction; $B5_{BA}$ and L_{PA}, Sterimol values describing steric effects from BA and the catalyst, respectively; and, i_{POsy}, the phosphate symmetric stretching intensity, which may represent the ability of each PA to engage in H-bonding/electrostatic interactions. Since previous attempts to model this entire data set were unsuccessful, these new NCI parameters provided the missing information for describing key influences in this complex reaction. More importantly, these results suggest that these parameters may provide a powerful platform for uncovering subtle NCIs, even when limited mechanistic/structural knowledge is available.

In order to further leverage this statistical physical organic strategy, a computational TS analysis for this reaction was performed at the ωB97X-D/def2-TZVPP/SMD(toluene)//ωB97X-D/6-31G(d) level of theory. The combinations of PA **6** with 4-Me-PhB(OH)$_2$ and 3,5-(MeO)$_2$-PhB(OH)$_2$ were selected as case studies as these groups gave divergent enantioselectivities (Figure 3A). First, a comprehensive conformational search at the TS level was performed for the PA **6**/4-Me-PhB(OH)$_2$ system. Remarkably, this DFT study revealed that TSs presenting a T-shaped NCI between the aryl ring of the BA and the binaphthyl moiety of the PA catalyst are the lowest in energy.[18] The favored TSs leading to the R and S products are depicted in Figure 4A, with **TS1-(R)** leading to the major observed product (computed $\Delta\Delta G^{\ddagger}$ = 1.0 kcal/mol; experimental $\Delta\Delta G^{\ddagger}$ = 0.9 kcal/mol). Location of low-lying TSs was also performed for the PA **6**/3,5-(MeO)$_2$-PhB(OH)$_2$ system. The analysis showed that **TS2-(R)** and **TS2-(S)** (Figure 4B) are the lowest in energy, and the formation of the S enantiomer as the major product is consistent with the observed results (computed $\Delta\Delta G^{\ddagger}$ = 2.6 kcal/mol; experimental $\Delta\Delta G^{\ddagger}$ = 1.2 kcal/mol). Supporting the hypothesis resulting from the parameters found in the statistical analysis, T-shaped π

interactions between the meta substituent of the BA and the binaphthyl moiety of the catalyst are present in both systems (Figure 4), and the computed distances between the aryl ring of the BA and the binaphthyl moiety of the catalyst are in good agreement with the calculated $^TD\pi_w$ parameters. Additional TS computations for the PA **6**/3-OMe-Ph-B(OH)$_2$ system, as an example of an asymmetrically substituted BA, are consistent with these results and are reported in the SI.

Although the data reported provide clear support for the proposed T-shaped interaction as an important influence in the enantiodiscrimination process, it is not trivial to explicitly understand its origin from the calculated TSs. Indeed, the conformations assumed by the catalyst−reagent adducts in the TSs are similar even when the BA is altered (compare **TS1-(R)** with **TS2-(R)** and **TS1-(S)** with **TS2-(S)**). Nonetheless, an advantage of merging TS calculations with the data set analyses is the ability to harness the experimental and computational information simultaneously. For example, the interactions that stabilize the BA−PA complex are conserved in each TS, including H-bonding (**a**), π stacking (**b**), and electrostatics (**c**) (Figure 4), which can be connected to the parameters i_{POsy} (**a** and **c**), and $^TD\pi_w$ and $B5_{BA}$ (**b**).

Further information can also be interpreted from the model and related back to the TSs, allowing for the proposal of a stereochemical model (Figure 4). As an example, the term L_{PA} (the length of the PA's aryl group) appears twice in the model and increases in the order **8 > 5 > 6 > 7**, which supports the significance of the size of the para substituent in the enantiodetermining step. Since this parameter is also present as a cross term with $^TD\pi_w$, it suggests that these two terms are interrelated in the TS. Accordingly, if the BA is farther from the binaphthyl group with a longer $^TD\pi_w$, as is the case with 3,5-disubstituted BAs, the alkene is driven toward the PA's aryl rings (Figure 4B). As a result, the alkene will rotate to minimize steric effects (**d**) between its bulkier substituent (Ph) and the para substituent on the PA, leading to favored fluorination at the alkene's Re face (Figure 4B). This observation is consistent with

the optimized reaction conditions previously reported, in which the best PA catalyst, **AdDIP** (i.e., 2,6-(iPr)$_2$-4-Ad-Ph), contains an adamantyl (Ad) group at the para position.[17a] Conversely, when a 3,5-unsubstituted BA is used, $^{T}D\pi_w$ is shorter, situating the alkene away from the PA's para substituent. In this case, the alkene may rotate to position either the Me or Ph group toward the PA with limited repulsion. This is consistent with the observation that 3,5-unsubstituted BAs generally afford lower enantioselectivity. To rationalize the inversion of stereoselection in certain examples (e.g., 4-Me-PhB(OH)$_2$), it is possible that the alkene's Ph group engages in a CH−π interaction (**e**) with the 4-alkyl moieties, thus stabilizing this conformation and allowing fluorination at the alkene's *Si* face (Figure 4A). Overall, combining detailed insight from the two methods provides a rationalization for a diverse set of results in a complex reaction, further validating the new parameters as descriptors of NCIs occurring in the TS.

In conclusion, the need for new tools to identify and quantify NCIs in catalysis prompted us to develop new parameters for describing π interactions: $E\pi$ and $D\pi$. These easily calculated parameters have been tested in two different catalytic systems using multivariate correlations. The obtained information agreed with previously reported studies in Birman's kinetic resolution of benzyl alcohols by supporting the occurrence of a π-stacking interaction. These parameters also provided detailed insight into a complex reaction, namely, the fluorination of allylic alcohols. Indeed, for this catalytic system the obtained model facilitated the identification of interactions occurring in the computed TSs. Thus, this new class of parameters provides a valuable extension to developing structure−function relationships by describing weak yet significant interactions occurring in the reaction. As shown, the use of $E\pi$ and $D\pi$ in multidimensional analysis offers a broad perspective of a reaction that can be distilled into a mathematical equation, directly relating the parameters to a TS structure. Hence, this methodology offers the opportunity to validate TS analyses through a set of experimental data. We see it as a complementary strategy to rigorous TS computations, both of which inform the nature of potential NCIs. We are currently integrating these approaches in ongoing projects as well as exploring the application of this strategy to other NCIs such as electrostatics and dispersion forces.

ASSOCIATED CONTENT

Ⓢ Supporting Information

The Supporting Information is available free of charge on the ACS Publications website at DOI: 10.1021/jacs.7b02311.

Experimental and modeling details, table of parameters, and DFT energies and geometries (PDF)

AUTHOR INFORMATION

Corresponding Authors

*fdtoste@berkeley.edu
*sigman@chem.utah.edu

ORCID

F. Dean Toste: 0000-0001-8018-2198
Matthew S. Sigman: 0000-0002-5746-8830

Notes

The authors declare no competing financial interest.

REFERENCES

(1) (a) Biedermann, F.; Schneider, H.-J. *Chem. Rev.* **2016**, *116*, 5216. (b) Neel, A.; Hilton, M. J.; Sigman, M. S.; Toste, F. D. *Nature* **2017**, *543*, 637. (c) Wagner, J. P.; Schreiner, P. R. *Angew. Chem., Int. Ed.* **2015**, *54*, 12274.

(2) (a) Johnson, E. R.; Keinan, S.; Mori-Sánchez, P.; Contreras-García, J.; Cohen, A. J.; Yang, W. *J. Am. Chem. Soc.* **2010**, *132*, 6498. (b) Krenske, E. H.; Houk, K. N. *Acc. Chem. Res.* **2013**, *46*, 979. (c) Seguin, T. J.; Wheeler, S. E. *ACS Catal.* **2016**, *6*, 7222. (d) Seguin, T. J.; Wheeler, S. E. *Angew. Chem., Int. Ed.* **2016**, *55*, 15889.

(3) (a) Harper, K. C.; Sigman, M. S. *Science* **2011**, *333*, 1875. (b) Sigman, M. S.; Harper, K. C.; Bess, E. N.; Milo, A. *Acc. Chem. Res.* **2016**, *49*, 1292.

(4) Zhang, C.; Santiago, C. B.; Crawford, J. M.; Sigman, M. S. *J. Am. Chem. Soc.* **2015**, *137*, 15668.

(5) (a) Bess, E. N.; Guptill, D. M.; Davies, H. M. L.; Sigman, M. S. *Chem. Sci.* **2015**, *6*, 3057. (b) Niemeyer, Z. L.; Milo, A.; Hickey, D. P.; Sigman, M. S. *Nat. Chem.* **2016**, *8*, 610.

(6) Milo, A.; Neel, A. J.; Toste, F. D.; Sigman, M. S. *Science* **2015**, *347*, 737.

(7) Mougel, V.; Santiago, C. B.; Zhizhko, P. A.; Bess, E. N.; Varga, J.; Frater, G.; Sigman, M. S.; Copéret, C. *J. Am. Chem. Soc.* **2015**, *137*, 6699.

(8) Harper, K. C.; Bess, E. N.; Sigman, M. S. *Nat. Chem.* **2012**, *4*, 366.

(9) Knowles, R. R.; Jacobsen, E. N. *Proc. Natl. Acad. Sci. U. S. A.* **2010**, *107*, 20678.

(10) (a) Chen, Z.-M.; Hilton, M. J.; Sigman, M. S. *J. Am. Chem. Soc.* **2016**, *138*, 11461. (b) Yamamoto, E.; Hilton, M. J.; Orlandi, M.; Saini, V.; Toste, F. D.; Sigman, M. S. *J. Am. Chem. Soc.* **2016**, *138*, 15877.

(11) Knowles, R. R.; Lin, S.; Jacobsen, E. N. *J. Am. Chem. Soc.* **2010**, *132*, 5030.

(12) (a) Gamez, P.; Mooibroek, T. J.; Teat, S. J.; Reedijk. *Acc. Chem. Res.* **2007**, *40*, 435. (b) Bloom, J. W. G.; Wheeler, S. E. *Angew. Chem., Int. Ed.* **2011**, *50*, 7847. (c) Bloom, J. W. G.; Raju, R. K.; Wheeler, S. E. *J. Chem. Theory Comput.* **2012**, *8*, 3167. (d) Dougherty, D. A. *Acc. Chem. Res.* **2013**, *46*, 885. (e) Karthikeyan, S.; Ramanathan, V.; Mishra, B. K. *J. Phys. Chem. A* **2013**, *117*, 6687. (f) Cozzi, F.; Cinquini, M.; Annuziata, R.; Siegel, J. S. *J. Am. Chem. Soc.* **1993**, *115*, 5330. (g) Cockroft, S. L.; Hunter, C. A.; Lawson, K. R.; Perkins, J.; Urch, C. J. *J. Am. Chem. Soc.* **2005**, *127*, 8594. (h) Gung, B. W.; Xue, X.; Reich, H. J. *J. Org. Chem.* **2005**, *70*, 3641. (i) Cockroft, S. L.; Hunter, C. A. *Chem. Soc. Rev.* **2007**, *36*, 172. (j) Hwang, J.; Li, P.; Carroll, W. R.; Smith, M. D.; Pellechia, P. J.; Shimizu, K. D. *J. Am. Chem. Soc.* **2014**, *136*, 14060. (k) Martinez, C. R.; Iverson, B. L. *Chem. Sci.* **2012**, *3*, 2191.

(13) (a) Wheeler, S. E.; Houk, K. N. *J. Am. Chem. Soc.* **2008**, *130*, 10854. (b) Wheeler, S. E. *Acc. Chem. Res.* **2013**, *46*, 1029.

(14) Wheeler, S. E. *J. Am. Chem. Soc.* **2011**, *133*, 10262.

(15) (a) Birman, V. B.; Uffman, E. W.; Jiang, H.; Li, X.; Kilbane, C. J. *J. Am. Chem. Soc.* **2004**, *126*, 12226. (b) Birman, V. B.; Jiang, H. *Org. Lett.* **2005**, *7*, 3445.

(16) Li, X.; Liu, P.; Houk, K. N.; Birman, V. B. *J. Am. Chem. Soc.* **2008**, *130*, 13836.

(17) (a) Zi, W.; Wang, Y.-M.; Toste, F. D. *J. Am. Chem. Soc.* **2014**, *136*, 12864. (b) Neel, A. J.; Milo, A.; Sigman, M. S.; Toste, F. D. *J. Am. Chem. Soc.* **2016**, *138*, 3863.

(18) (a) Greindl, J.; Hioe, J.; Sorgenfrei, N.; Morana, F.; Gschwind, R. M. *J. Am. Chem. Soc.* **2016**, *138*, 15965. (b) Sorgenfrei, N.; Hioe, J.; Greindl, J.; Rothermel, K.; Morana, F.; Lokesh, N.; Gschwind, R. M. *J. Am. Chem. Soc.* **2016**, *138*, 16345.